

Energy Band Gap Investigation using First Principle Simulation and Tauc Plot Method of Calixarene and Calixarene-Drug Inclusion Complexes

Nur Farah Nadia Abd Karim¹, Faridah Lisa Supian^{1*}, Wong Yeong Yi¹,
Afiq Radzwan¹, Mazlina Musa², Amiruddin Shaari³, Abdullah F. Al Naim⁴

¹Department of Physics, Faculty of Science and Mathematics, Universiti Pendidikan Sultan Idris, 35900 Tanjong Malim, Perak, Malaysia

²Department of Chemistry, Faculty of Science and Mathematics, Universiti Pendidikan Sultan Idris, 35900 Tanjong Malim, Perak, Malaysia

³Department of Physics, Faculty of Science, Universiti Teknologi Malaysia, 81310 Skudai, Johor Bahru, Johor, Malaysia

⁴Department of Physics, College of Science, King Faisal University, Saudi Arabia

*Corresponding author: faridah.lisa@fsm.ups.edu.my

Received: June 2023; **Published:** November 2023

ABSTRACT

Calixarene has attract attention especially in drug delivery and drug sensor systems due to its peculiar properties, such as functional diversity of the upper and lower rims, hydrophobic cavity, chemical stability, zero toxicity, and controlled release profile. These properties make this supramolecule an ideal candidate for drug encapsulation and sensors. P-aminobenzoic acid (PABA) is a drug in sunscreen which is widely used as a ultraviolet (UV) filter and sunburn protector to protect against solar rays. The calix[n]arene (n=4,6,8) and the host-guest interaction of calix[n]-PABA were characterized using UV-visible spectroscopy and the first-principles pseudopotential method, based on the density functional theory (DFT) and the plane-wave method as implemented into Quantum Espresso code. The DFT calculation is performed to find the estimated calix[n]arene and calix[n]arene-drug band gap. The band gap calculated using DFT has usually underestimated the insulating materials for about 30 – 50% of the experimental gap values, depending on the selected type of exchange-correlation chosen. The optical band gap value of calix[n]arene and calix[n]-PABA obtained from the UV-Visible absorption spectrum estimated using the Tauc plot are then compared with the band gap computed by DFT. The band gap narrowing shown by the complexes indicates that calix[n]arene and PABA reacted. Besides, calix[8]arene is the most promising host in this study since the calix[8]-PABA complex has the most significant binding energy. The band gaps and binding energy results will become a reference for future research in calixarene and calixarene-drug material.

Keywords: Band gap, Calixarene, DFT, PABA, Quantum Espresso, Tauc relation, UV-Visible

1. INTRODUCTION

4-aminobenzoic acid or para-aminobenzoic acid (PABA) consists of carboxyl and amino groups opposite to one another in para-position with a formula of $C_7H_7NO_2$ as shown in Figure 1. PABA has multiple antiviral and antioxidant properties, making this substance an active substance in sunscreen for ultraviolet (UV) B irradiation protection (Ma & Yoo, 2021).

PABA is a pioneer patented sunscreen and is most widely used as a UV filter (Chan et al., 2020) to serve as a sunburn protectant (Guan et al., 2021; Shanuja et al., 2018) against UVB radiation. In addition, it also protects against the harmful effects of solar radiation, such as DNA

damage, skin aging, and even skin cancer (Han et al., 2020). Many methods have been established to synthesize and characterize nanosensors (Ayoubi-Chianeh & Kassae, 2020). However, developing a susceptible nanosensor and maintaining a drug's structure intact is challenging (Ayoubi-Chianeh & Kassae, 2020).

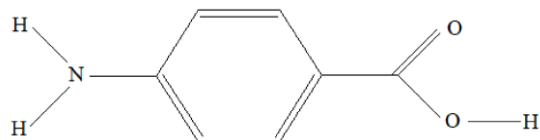


Figure 1. Chemical Structure of 4-aminobenzoic acid

Currently, the development of sensor materials that provide specific and sensitive results for analyzing chemical compounds as guests in host inclusion complexes is actively carried out. In this view, calixarene-based nanosensors have been reported to display significant responses towards various guest molecules such as cation (Supian et al., 2022), anion (Edwards et al., 2021), and neutral molecule (Fort & Scott, 2016) based on the optimized structural and geometrical factors (Panchal et al., 2020). Furthermore, calixarene can remarkably act as a receptor for trapping or encapsulating chemical entities (Gassoumi et al., 2019), forming host-guest complexes, which continuously increases the interest as a significant host molecule in many fields of supramolecular chemistry (Fahmy et al., 2020), particularly in drug delivery and drug sensor systems (Yuksel et al., 2021).

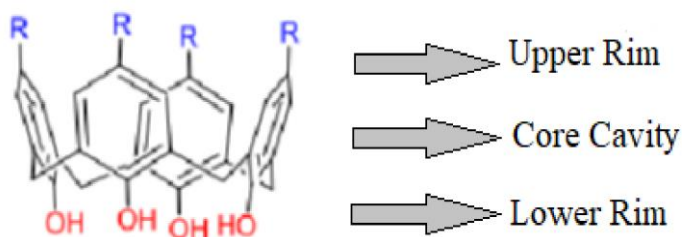


Figure 2. Structure of calix[4]arene (Español & Villamil, 2019)

Calixarene is an ideal host molecule for various therapeutic guest drugs due to its unique architecture macromolecule composed of an upper rim with a para-substituent phenolic ring, a lower rim with a phenolic hydroxyl group, and a hydrophobic π electron-rich core cavity (Figure 2). Furthermore, other promising properties of calixarene, such as chemical stability, hydrophobic cavity, zero toxicity, and controlled release profiles, have made this material fit as an adsorbent and sensor for drugs (Español & Villamil, 2019). In addition, the ability of calixarene as a drug carrier for cancer treatment has been proven several times (Liu et al., 2021; Wang et al., 2022; Xu et al., 2022).

To our knowledge, there are limited reports on the calixarene-based nanosensors for PABA drug detection. Herein, we investigate the band gap between calixarene, PABA, and calixarene-PABA host-guest inclusion. The calix[n]arene ($n = 4,6,8$) have been chosen as hosts in this study. Determination of the interaction between the calixarene-based nanosensor and the PABA drug guest was studied using ultraviolet visible spectroscopy (UV-Vis) and Density Functional Theory (DFT). Moreover, the binding energy of the complexes was also evaluated to determine the most optimal host for PABA drugs and to study the stability of the calix[n]-PABA inclusion complex.

2. MATERIALS AND METHODS

2.1. Materials

Three types of calixarene which is 25, 26, 27, 28- tetrahydroxycalix[4]arene (C4), Calix[6]arene-37,38,39,40,41,42-hexol (C6) and 49, 50, 51, 52, 53, 54, 55, 56-octahydroxycalix[8]arene (C8) were used and purchased from Sigma-Aldrich. The PABA drug with the empirical formula of C₇H₇NO₂ and molecular weight of 137.14 g/mol was purchased from Bendosen.

2.2. Methodology

2.2.1. Optical measurement

The spectral studies of all sample were carried out as follow: 0.2mg/mol concentration of calix[n]arene diluted with chloroform and PABA diluted with deionized water with the concentration of 50µl/ml according to the PABA standard solution concentration (Salvador et al., 2003). Host-guest complexes follow a 1:1 molar ratio (Fahmy et al., 2020). The optical properties of calixarene, PABA, and calix-PABA solution were studied using Agilent 8453 UV-Visible spectroscopy with a wavelength ranging from 190 to 1100nm. The absorption coefficient, α of the sample solution, was determined using the approximate expression 1 (Leontie et al., 2018):

$$\alpha = \frac{1}{0.4343 l} \ln \frac{I_0}{I} \quad (1)$$

where l is the length of the cuvette, 1cm, and I_0 and I are the intensity of the incident and emergent beams. The effect of reflection of photon energies, $h\nu$ that is less than the optical band gap, is neglected (Leontie et al., 2018).

2.2.2. Computational calculation

The theoretical calculations were performed using the first-principles pseudopotential method, based on the principle of the density functional theory (DFT) proposed by famous Hohenberg and Kohn (Hohenberg & Kohn, 1964; Kohn & Sham, 1965; Sham & Schlüter, 1983) and the plane-wave method implemented in Quantum Espresso code (Giannozzi et al., 2009). The exchange-correlation functional, which is the generalized-gradient-approximation (GGA) with the parametrizations of Perdew–Berke–Erzndof (PBE) (Perdew et al., 1996), is chosen to treat electron-electron interaction as the exchange-correlation functional for geometry optimization (Borlido et al., 2020; Lawal et al., 2017). The ultrasoft pseudopotentials (USPP) method in the form of Rappe Rabe Kaxiras Joannopoulos ultra-soft (rrkjus) was applied to treat the electron-ion core interactions (Rappe et al., 1990). Furthermore, the Born-Oppenheimer approximation is used to split the movement of nuclei and electrons to perform geometry optimization calculations (Schlegel, 2011) to determine cell dimensions and optimal atomic positions (lowest energy). The Broyden-Fletcher-Goldfarb-Shanno (BFGS) algorithm is chosen to solve the geometry optimization. In optimization calculation, the maximum atomic forces are lowered than the threshold of 1.0×10^{-3} Ry/Bohr. To calculate the self-consistent field (SCF), a set of (2×1×1) Monkhorst-Pack grids is used to sample the irreducible Brillouin zone to generate k-points. The electron wave functions and charge density are expanded using the plane-wave basis set with kinetic energy cutoffs of 25 Ry and 225 Ry, respectively. The SCF

convergence threshold is set to 1×10^{-6} Ry. The complexes' binding energy can be determined from SCF (Bagus et al., 2019). According to Neopane and Pantha (2019), the binding energy is the change of the system's ground state energy and the optimal position energy of the molecules in the system (Neopane & Pantha, 2019). Thus, the binding energy of the calix[n]-PABA complexes was then obtained according to the following equation (Panchal et al., 2020):

$$\Delta E_{\text{bind}} = E_{\text{Complex}} - (E_{\text{host}} + E_{\text{guest}}) \quad (2)$$

The binding energy indicates the stability of the structure; the structure is proved to be more stable when the binding energy is more negative (Kandeel et al., 2021). Furthermore, the selectivity of the appropriate host to respect drug binding can be estimated (Athar et al., 2018). Figure 3 shows the host-guest structure obtained from DFT software.

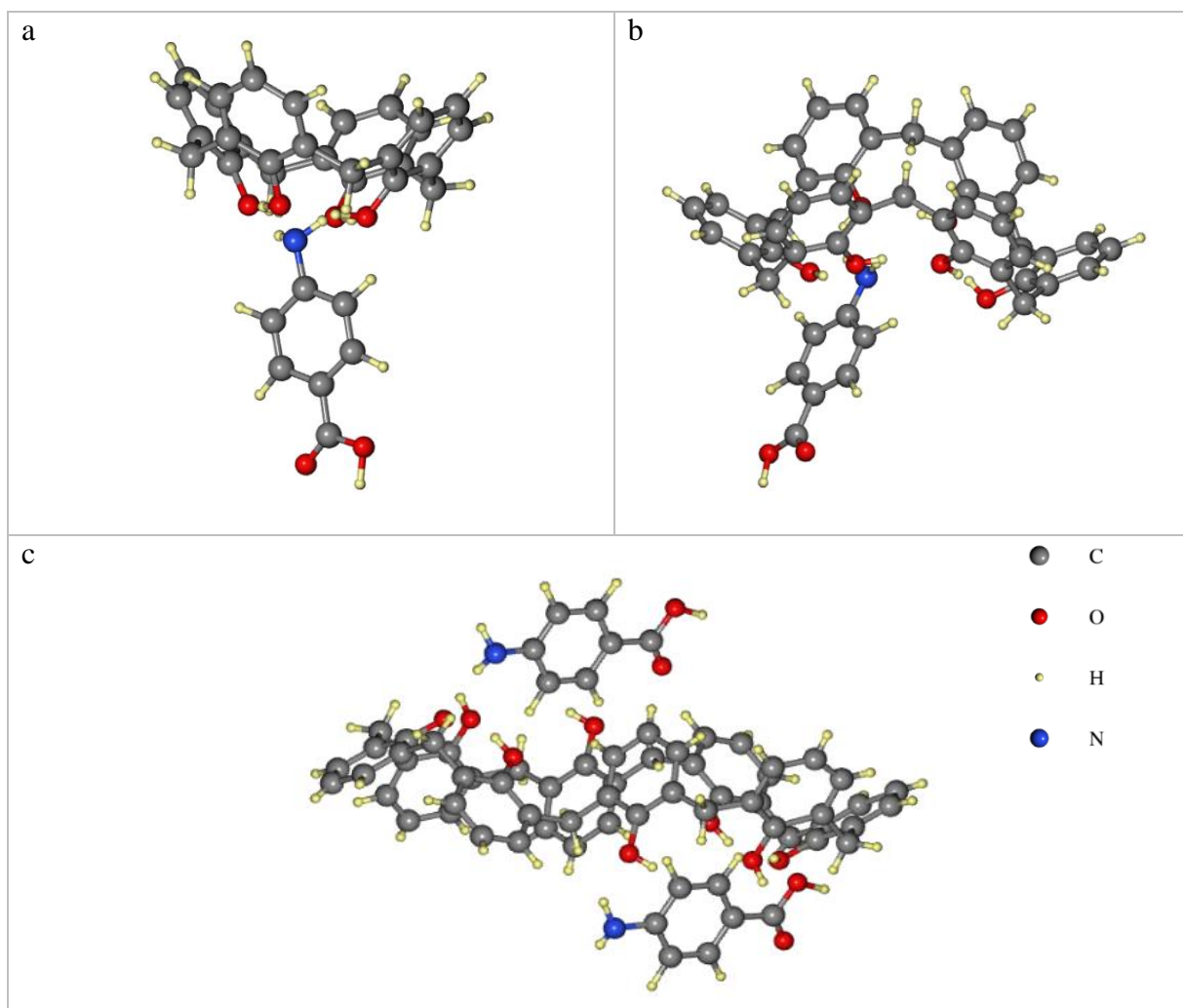


Figure 3. The host-guest complexes (a) calix[4]-PABA, (b) calix[6]-PABA and (c) calix[8]-PABA

3. RESULTS AND DISCUSSION

3.1. Optical characterization

The optical band gap of a molecule is the energy of the lowest electronic transition accessible via absorption of a single photon (Bredas, 2014). Therefore, the energy band gap of

a molecule determined by absorption spectra is more appropriate (Leontie et al., 2018). The experimental value of the energy band gap is determined by the Tauc relation, where the energy-dependent absorption coefficient α can be expressed as follow (Leontie et al., 2018);

$$\alpha hv = A(hv - E_{go})^n \quad (3)$$

where $n = 1/2$ or 2 for optical direct or indirect allowed transitions, E_{go} is the optical band gap, and A is a constant. The value of n can be determined by plotting the $(\alpha hv)^n$ versus energy, $h\nu$. The best fit graph for the extrapolation x-axis will reveal the correct transition type. In this work, $n = 2$, indirect transitions band gap is used. Moreover, the optical band gap value is determined by extrapolating straight lines to αhv equal to 0. The optical absorption of molecules and complexes is shown in Figure 4.

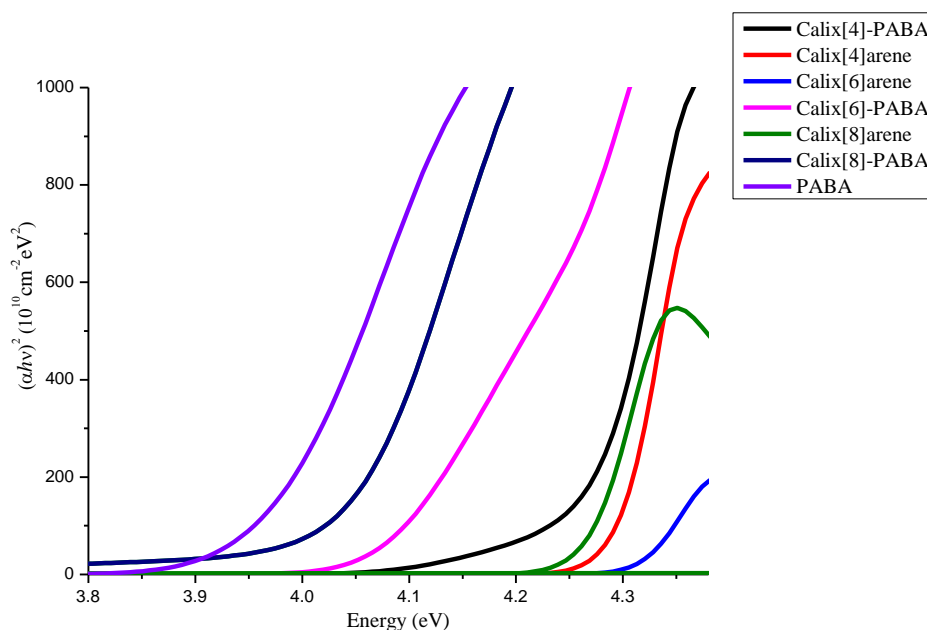


Figure 4. The absorption spectra of present calix[n]arene and calix[n]-PABA

Table 1 represents the optical band gap of all samples. The band gap value of calixarene is high, showing that it is highly insulating in electrical conductivity (Lim & Supian, 2020). However, the calixarene and PABA band gap value decrease when forming host-guest complexes, indicating an interaction between calixarene as a host sensing the PABA guest. This host-guest complex formation may change the charge distributions, the electronic structures, and the energy gaps of the pure molecules (Liu et al., 2020). Furthermore, the optical band gap of the host-guest complexes decreases as the phenolic units of calixarene increase. The reduction in band gap shows that the complex has low kinetic stability yet provides better electric conduction (Jang et al., 2018).

Table 1. The optical band gap value of PABA, calix[n]arene and calix[n]-PABA

Sample	Optical band gap (eV)
PABA	3.97
Calix[4]arene	4.30
Calix[4]-PABA	4.27
Calix[6]arene	4.32
Calix[6]-PABA	4.16
Calix[8]arene	4.27
Calix[8]-PABA	4.03

3.2. Computational studies

The energy band gap of the samples calculated using DFT is tabulated in Table 2. The band gap computed by DFT has the same trend as the Tauc plot estimation, where the band gap of calixarene and PABA decreases when forming host-guest inclusion. It confirms that the drug guest, PABA incorporation into calix[n]arene can induce the noticeable band gap narrowing consistent with the experimental result (Mingzhu et al., 2013). However, the band gap's theoretical value is lower than the experimental gap as the exchange-correlation potential treated with Perdew-Burke-Ernzerhof (PBE) underestimates the band gap of the insulating materials (García et al., 2017). The electronic gap from GGA typically underestimates experimental gap values for insulating materials by about 30– 50% (Kolos & Karlický, 2019). Hence, the actual value of the sample band gap should be greater than the calculated value.

Table 2. The energy band gap value of PABA, calix[n]arene and calix[n]-PABA

Molecule/ Complex	Energy band gap (eV)
PABA	3.27
Calix[4]arene	3.69
Calix[4]-PABA	2.81
Calix[6]arene	3.86
Calix[6]-PABA	2.64
Calix[8]arene	2.38
Calix[8]-PABA	1.37

The binding energy of all three host-guest complexes is shown in Table 3. The binding energy is calculated according to the 1:1 binding stoichiometric for calix[4]arene and calix[6]arene (Fahmy et al., 2020) and 1:2 for calix[8]arene to drug ratio (Moussa et al., 2018). For smaller calix[n]arene, n=4,6 can only accommodate one drug molecule in the cavity, whereas n>6 can hold two drug molecules within a single macrocycle (Moussa et al., 2018). The calix[8]-PABA inclusion has the highest binding energy, - 0.06189492 Ry, compared with the other two host-guest complexes; reveals PABA can generate optimal complexes with calix[8]arene (Kandeel et al., 2021). These findings prove that the calix[n] arene's core cavity size affects its binding capability, which agrees with work that was experimented on by Athar et al. in 2018 (Athar et al., 2018).

Table 3. The binding energy of calix[n]-PABA

Molecule/ Complex	Binding Energy (Ry)
Calix[4]arene-PABA	-0.00744111
Calix[6]arene-PABA	-0.00697114
Calix[8]arene-PABA	-0.06189492

4. CONCLUSION

The band gap of the calix[n]arenes and PABA molecules and the calix[n]-PABA inclusion complexes were determined using the Tauc plot and computational method. Both studies significantly reduce the pure molecule's band gap when forming a host-guest inclusion. This phenomenon confirms an interaction between the calix[n]arene as host and PABA guest molecules. Moreover, the narrowing band gap trend proves that calix[n]arene can shift its properties from insulating to semiconductor organic material with suitable derivatives added at both rims. The binding energy findings reveal that the core cavity size of the calix[n]arene affects its binding ability. Since the calix[8]arene have the largest cavity compared to the other two hosts, it has the highest binding energy, which indicates that it is an excellent host for PABA drug guests in this experiment.

Acknowledgement

The authors would like to express their deepest gratitude to the Fundamentals Research Grant Scheme (FRGS: 2020-0256-103-02) from the Ministry of Higher Education and the Universiti Pendidikan Sultan Idris (UPSI) for supporting the research.

REFERENCES

- Athar M, Ranjan P, Jha PC. (2018). Investigation of calixarene complexes with dasatinib and lapatinib: A Density Functional Theory approach. *Journal of Inclusion Phenomena and Macrocyclic Chemistry*, 84, 160-165.
- Ayoubi-Chianeh M, Kassaei MZ. (2020). Detection of bendamustine anti-cancer drug via AlN and Si-doped C nanocone and nanosheet sensors by DFT. *Structural Chemistry*, 31(5), 2041-2050.
- Bagus PS, Nelin CJ, Zhao X, Levchenko SV, Davis E, Weng X, Späth F, Papp C, Kuhlenbeck H, Freund HJ. (2019). Revisiting surface core-level shifts for ionic compounds. *Physical Review B*, 100(11), 1-5.
- Borlido P, Schmidt J, Huran AW, Tran F, Marques MAL. (2020). Exchange-correlation functionals for band gaps of solids: benchmark, reparametrization and machine learning. *Npj Computational Materials*, 6(1), 1-17.
- Bredas JL. (2014). Mind the gap! *Materials Horizons*, 1(1), 17-19.
- Chan CTL, Ma C, Chan RCT, Ou HM, Xie HX, Wong AKW, Wang ML, Kwok WM. (2020). A long lasting sunscreen controversy of 4-aminobenzoic acid and 4-dimethylaminobenzaldehyde derivatives resolved by ultrafast spectroscopy combined with density functional theoretical study. *Physical Chemistry Chemical Physics*, 22(15), 8006-8020.
- Edwards NY, Schnable DM, Gearba-dolocan IR, Strubhar JL. (2021). Terpyridine-Functionalized Calixarenes: Synthesis, Characterization and Anion Sensing Applications. *Molecules*, 26, 87.
- Español ES, Villamil MM. (2019). Calixarenes: Generalities and their role in improving the solubility, biocompatibility, stability, bioavailability, detection, and transport of biomolecules. *Biomolecules*, 9(3), 90.
- Fahmy SA, Ponte F, Fawzy IM, Sicilia E, Bakowsky U, Azzazy HMES. (2020). Host-guest complexation of oxaliplatin and para-sulfonatocalix[n]arenes for potential use in cancer therapy. *Molecules*, 25(24), 5926.
- Fort EH, Scott LT. (2016). Selective Recognition of Neutral Guests in an Aqueous Medium by a Biomimetic Calix[6]cryptamide Receptor. *Organic and Biomolecular Chemistry*, 14(30), 738-746.
- García ÁM, Valero R, Illas F. (2017). An Empirical, Yet Practical Way to Predict the Band Gap in Solids by Using Density Functional Band Structure Calculations An empirical , yet practical way to predict the band gap in solids by using density functional band structure calculations. *Journal of Physical Chemistry C*, 121, 18862-18866.
- Gassoumi B, Ghalla H, Chaabane RB. (2019). DFT and TD-DFT investigation of calix[4]arene interactions with TFSI-ion. *Heliyon*, 5(11), e02822.
- Giannozzi P, Baroni S, Bonini N, Calandra M, Car R, Cavazzoni C, Ceresoli D, Chiarotti GL, Cococcioni M, Dabo I, Dal Corso A, De Gironcoli S, Fabris S, Fratesi G, Gebauer R, Gerstmann U, Gougoussis C, Kokalj A, Lazzeri M, Wentzcovitch RM. (2009). Quantum Espresso: A modular and open-source software project for quantum simulations of materials. *Journal of Physics Condensed Matter*, 21(39), 1-19.
- Guan LL, Lim HW, Mohammad TF. (2021). A Review of Current Literature Sunscreens and Photoaging : A Review of Current Literature. *American Journal of Clinical Dermatology*, 22, 819-828.
- Han C, Yang H, Li B, Wang Z. (2020). Exogenous pyruvate facilitates ultraviolet B-induced DNA damage repair by promoting H3K9 acetylation in keratinocytes and melanocytes. *Biomedicine and Pharmacotherapy*, 126, 110082.
- Hohenberg P, Kohn W. (1964). Inhomogeneous Electron Gas. *Physical Review*, 136, 864-871.
- Jang YM, Yu CJ, Kim JS, Kim SU. (2018). Ab initio design of drug carriers for zoledronate guest molecule using phosphonated and sulfonated calix[4]arene and calix[4]resorcinarene host molecules. *Journal of Materials Science*, 53(7), 5125-5139.
- Kadhun WR, Oshizaka T, Ichiro H, Todo H, Sugibayashi K. (2016). Usefulness of liquid-crystal oral formulations to enhance the bioavailability and skin tissue targeting of p-amino benzoic acid as a model compound. *European Journal of Pharmaceutical Sciences*, 88, 282-290.
- Kandeel M, Abdelrahman AHM, Oh-Hashi K, Ibrahim A, Venugopala KN, Morsy MA, Ibrahim MAA. (2021). Repurposing of FDA-approved antivirals, antibiotics, anthelmintics, antioxidants, and cell protectives against SARS-CoV-2 papain-like protease. *Journal of Biomolecular Structure and Dynamics*, 39(14), 5129-5136.
- Kohn W, Sham LJ. (1965). Self-Consistent Equations Including Exchange and Correlation Effects. *Physical Review*, 140(4A), 1133-1138.
- Kolos M, Karlický F. (2019). Accurate many-body calculation of electronic and optical band gap of bulk hexagonal boron nitride. *Physical Chemistry Chemical Physics*, 21(7), 3999-4005.

- Lawal A, Shaari A, Ahmed R, Jarkoni N. (2017). First-principles investigations of electron-hole inclusion effects on optoelectronic properties of Bi₂Te₃, a topological insulator for broadband photodetector. *Physica B: Condensed Matter*, 520, 69-75.
- Leontie L, Danac R, Carlescu A, Doroftei C, Rusu GG, Tiron V, Gurlui S, Susu O. (2018). Electric and optical properties of some new functional lower-rim-substituted calixarene derivatives in thin films. *Applied Physics A: Materials Science and Processing*, 124(5), 1-12.
- Lim DCK, Supian FL. (2020). Langmuir, Raman, and electrical properties comparison of calixarene and calixarene-rGO using Langmuir Blodgett (LB) technique. *Journal of Materials Science: Materials in Electronics*, 31, 18487-18494.
- Liu D, Fan X, Dong D, Zhang Z, Yu N, Yang Z, Liu R, Liu B. (2020). Synthesis and high pressure studies of white luminescence host-guest complex nanocrystals based on C₆₀ and p-But-calix[8]arene. *Nanotechnology*, 31(16), 165701.
- Liu Q, Zhang TX, Zheng Y, Wang C, Kang Z, Zhao Y, Chai J, Li HB, Guo DS, Liu Y, Shi L. (2021). Calixarene-Embedded Nanoparticles for Interference-Free Gene-Drug Combination Cancer Therapy. *Small*, 17(8), 1-11.
- Ma Y, Yoo J. (2021). History of sunscreen: An updated view. *Journal of Cosmetic Dermatology*, 20(4), 1044-1049.
- Mingzhu L, Limei S, Shan W. (2013). First-principles study of electronic and optical properties in wurtzite ZnCo alloys. *Applied Mechanics and Materials*, 333, 1847-1852.
- Monkhorst H, Pack J. (1976). Special points for Brillouin zone integrations. *Physical Review B*, 13(12), 5188-5192.
- Moussa YE, Qing Y, Ong E, Perry JD, Cheng Z, Kayser V, Cruz E, Kim RR, Sciortino N, Wheate NJ. (2018). Demonstration of In Vitro Host-Guest Complex Formation and Safety of para -Sulfonatocalix [8] arene as a Delivery Vehicle for Two Antibiotic Drugs. *Journal of Pharmaceutical Sciences*, 1-7.
- Neopane S, Pantha N. (2019). First-Principles Study of Van Der Waals Interactions between Halogen Molecules (Cl₂ and I₂). *Journal of Nepal Physical Society*, 5(1), 19-23.
- Panchal M, Kongor A, Athar M, Modi K, Patel C, Dey S, Vora M, Bhadresha K, Rawal R, Jha PC, Jain VK. (2020). Structural motifs of oxacalix[4]arene for molecular recognition of nitroaromatic explosives: Experimental and computational investigations of host-guest complexes. *Journal of Molecular Liquids*, 306, 112809.
- Perdew JP, Burke K, Ernzerhof M. (1996). Generalized gradient approximation made simple. *Physical Review Letters*, 77(18), 3865-3868.
- Rappe AM, Rabe KM, Kaxiras E, Joannopoulos JD. (1990). Optimized pseudopotentials. *Physical Review B*, 41(2), 1227-1230.
- Salvador A, Chisvert A, Rodríguez A, March JG. (2003). Indirect spectrophotometric determination of p-aminobenzoic acid in sunscreen formulations by sequential injection analysis. *Analytica Chimica Acta*, 493(2), 233-239.
- Schlegel HB. (2011). Geometry optimization. *Wiley Interdisciplinary Reviews: Computational Molecular Science*, 1(5), 790-809.
- Sham LJ, Schlüter M. (1983). Density-Functional Theory of the Energy Gap. *Physical Review Letters*, 51(20), 1888-1891.
- Shanuja SK, Iswarya S, Gnanamani A. (2018). Marine fungal DHICA as a UVB protectant: Assessment under in vitro and in vivo conditions. *Journal of Photochemistry and Photobiology B: Biology*, 179, 139-148.
- Supian FL, Azahari NA, Juahir Y. (2022). Correlation of Langmuir Isotherm, Optical, Surface Potential and Morphological Characterizations of Two Functionalized Dihydroxycalix [4] arene for Lead Cation Entrapment. *Journal of Microscopy*, 1, 9-19.
- Wang C, Chang YX, Chen X, Bai L, Wang H, Pan YC, Zhang C, Guo DS, Xue X. (2022). A Calixarene Assembly Strategy of Combined Anti-Neuroinflammation and Drug Delivery Functions for Traumatic Brain Injury Therapy. *Molecules*, 27(9), 2967.
- Xu L, Chai J, Wang Y, Zhao X, Guo D, Shi L, Zhang Z, Liu Y. (2022). Calixarene-intergrated Nanodrug Delivery System for Tumor-targeted Delivery and Tracking of Anti-cancer Drugs In vivo. *Nano Research*, 15(8), 7295-7303.
- Yuksel N, Köse A, Fellah MF. (2021). The supramolecularly complexes of calix[4]arene derivatives toward favipiravir antiviral drug (used to treatment of COVID-19): a DFT study on the geometry optimization, electronic structure and infrared spectroscopy of adsorption and sensing. *Journal of Inclusion Phenomena and Macrocyclic Chemistry*, 101, 77-89.